Langmuir

Article

pubs.acs.org/Langmuir

A Gene-Networked Gel Matrix-Supported Lipid Bilayer as a Synthetic Nucleus System

Sun Ju Bae,[†] Woo Chul Song,[†] Sung Hwan Jung,[§] Seung-Woo Cho,[∥] Dong-Ik Kim,[⊥] and Soong Ho Um*[,†,‡]

[†]School of Chemical Engineering and [‡]SKKU Advanced Institute of Nanotechnology (SAINT), Sungkyunkwan University, Suwon, Gyeonggi-do, 440-760, South Korea

[§]Department of Engineering Science and Mechanics, Virginia Tech, Blacksburg, Virginia 24061, United States

[∥]Department of Biotechnology, Yonsei University, Seoul, 120-749, South Korea

[⊥]Division of Vascular Surgery, Samsung Medical Center, Sungkyunkwan University School of Medicine, Seoul, 135-710, South Korea

Supporting Information

ABSTRACT: A spheroidal transgene-networked gel matrix was designed as a synthetic nucleus system. It was spheroidically manufactured using both advanced lithography and DNA nanotechnology. Stable Aqueorea coerulescens green fluorescent protein (AcGFP)-encoding gene cross-networks have been optimized in various parameters: the number of gene-networked gel (G-net-gel) spheroids, the concentration of a AcGFP plasmid in the scaffold, and the molar ratio between the X-DNA building blocks and the gene. It was then assessed that 800 units of the gene networked gel matrix at a 4000:1 molar ratio of X-DNA blocks and AcGFP gene components accomplished 20-fold enhanced in vitro protein expression efficiency for 36 h. Furthermore, once with lipid capping, it reproduced the natural nucleus system, demonstrating the 2-fold increased levels of messenger RNAs (mRNAs) relative to solution phase vectors.

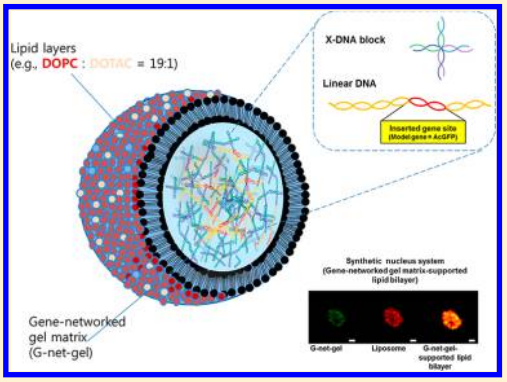

INTRODUCTION

Cells are three-dimensional multifunctional metabolic entities and are the principal subjects for biomimicry. With the advent of nanotechnology, the cell and its subdivisions, which include organelles, suborganelles, or complexes, have been modestly and artificially replicated.[1−10] At the same time, in addition to the rapid growth of genomics and proteomics, the development of a nucleus confined to a discrete, micrometer-scaled region is an emerging issue in this field, as the nucleus contains the genetic code. A three-dimensional nuclear structural model should consist of three major parts: a nuclear membrane, a nuclear transporter, and most importantly, chromatin.[11−13] In order to construct a synthetic nucleus, it is necessary to tightly connect and organize each gene at predetermined positions within a micrometer-sized area that has been enclosed by a lipid membrane. We sought to design a synthetic lipid-supported gene-networking gel matrix for use in a proto-nucleus system. Such a nucleus mimic system can be simply manufactured by linking exogenes via structural DNA nanotechnology and enclosing them with mixed lipid components.[14,15] We previously developed a DNA hydrogel system[16,17] composed of multiple copies of a single gene linked to the X-shaped DNA blocks that was fabricated in pad types. Combined with a coupled transcription−translation system, the gel system was proven to be able to act as an *in vitro* expression platform for a variety of protein groups. The gel scaffold contains a high concentration of genes, allows for a higher polymerase turnover rate, and protects DNA molecules by capping. By entrapping this system within outer lipid membrane components, a gene-networked gel matrix-supported lipid bilayer for a synthetic nucleus system can be easily achieved. Messenger RNA (mRNA) transcription was achieved using this system when transcription factors were included.

EXPERIMENTAL METHODS

Materials. All single-strand DNA was purchased from Integrated DNA Technology. X-DNA was synthesized as previously described.[16,17] The sequence information about the used X-DNA is described in the Supporting Information. pAcGFP vector was purchased from Clontech. pIVEX 1.3WG was purchased from 5PRIMES. All plasmid vectors were prepared through conventional subcloning methods.

Subcloning for the Preparation of Linear Plasmids. One-shot TOP10 chemically competent cells (*Escherichia coli*) were purchased from Invitrogen and used to amplify plasmids. AcGFP vector was digested at the Nco I and Stu I sites and inserted into the Nco I and Sma I sites of pIVEX 1.3WG to construct linear plasmids containing the AcGFP genes. The restriction site digest was confirmed through agarose gel electrophoresis. A QIAquick gel extraction kit (Qiagen)

Received: August 30, 2012
Revised: October 19, 2012

   dx.doi.org/10.1021/la303498k | *Langmuir* XXXX, XXX, XXX−XXX

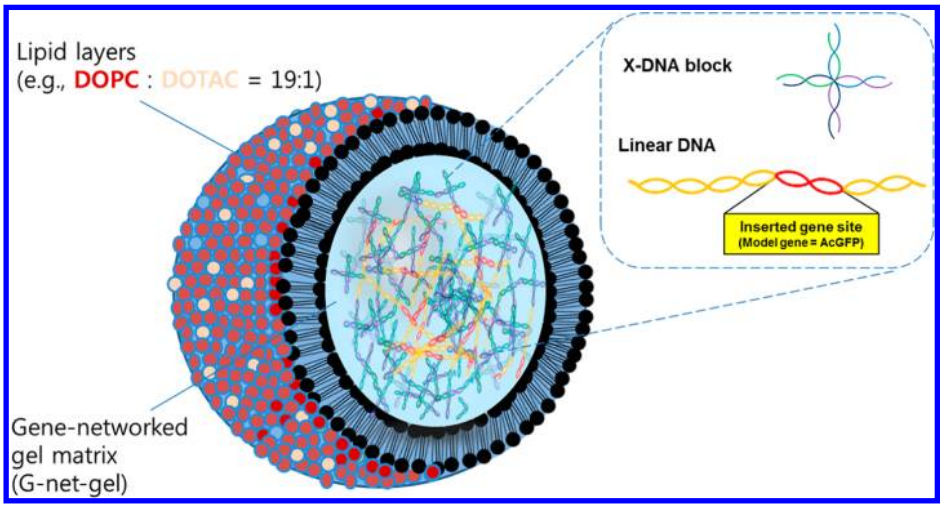

Figure 1. Schematic diagram of the synthetic nucleus system. The system is based on the combination of a G-net-gel as a core-nucleus and an outer lipid membrane.

was used for band extraction. pIVEX 1.3_AcGFP was obtained after a ligation process using T4 DNA ligase (Promega). The recombination vector pIVEX1.3_AcGFP was amplified by *E. coli* and then purified using a QIAprep Spin Miniprep kit (Qiagen). The amplified vectors were additionally cut at the Apa I sites to prepare linear plasmids. All restriction enzymes were purchased from New England Biolabs. All experiments related to cloning methods were executed following the procedures provided by the manufacturer.

Fabrication of Superhydrophobic Surfaces and the Circular Polydimethylsiloxane (PDMS) Mold. The superhydrophobicity design concept is inspired by the super-repulsion of water molecules on the surface of lotus leaves,[18−21] a process that involves a hydrophobic chemical in a patterned structure. To realize such a design, sapphire was used as a basic substrate. A sapphire substrate was purchased from Shinkosha. ZnO nanoparticles (20−200 nm in size) were deposited on the sapphire surface. A gold layer with a height of 5 nm was deposited on the ZnO surface using either E-beam lithography or sputtering. A superhydrophobic surface was produced using a heptadecafluoro-1-decanethiol (HDFT) solution for 15 min. Each layer was observed via a scanning electron microscopic tool (see Figure S1, Supporting Information). For microfabrication of PDMS, a negative photomask was produced in 15 × 15 arrays with a circular pattern (diameter = 100 μm). Circular patterns on the PDMS mold were achieved using standard UV photolithography (see Figure S2 for more detail). The HDFT concentration and incubation time were optimized to obtain the most suitable superhydrophobic surface. In these experiments, optimal superhydrophobicity was achieved at a HDFT concentration of 1 mM regardless of the nanoparticle arraying method (Figure S3).

Optimization of the Microscaled Gene-Networked Gel (G-net-gel). The gel precursor was composed of X-DNA blocks, linear plasmids, and T4 DNA ligase (Promega). An X-DNA/plasmid ratio of 4000:1 was achieved with a mixture of 70 μM of X-DNA and 17.5 nM of plasmid. Manufactured G-net-gel precursor solutions were dropped onto the superhydrophobic surfaces, immediately covered by a circular PDMS mold, and cured for 4 h at room temperature.

Confocal Microscopic Imaging. In order to obtain fluorescence microscopic images, all G-net-gels were stained with 100x SYBR green I dye (Invitrogen). Texas Red DHPE (Invitrogen) was used for lipid staining. For fixation of the samples for microscopic observation, slides were coated with cationic agents, calcium chloride solution, and an alginate solution (Sigma).

Protein Expression. For protein expression, wheat-germ lysates (RTS 100 Wheat germ CECF kits) were purchased from 5PRIME and reacted as recommended by the manufacturer. Relative fluorescence units (RFUs) were measured by sampling AcGFP. RFU values were converted to the concentration of active protein based on an AcGFP standard (2.1×10^7 RFU/mg).

Preparation of the Proto-nucleus System. For the G-net-gel matrix-supported lipid bilayer, all lipid components (e.g., 1,2-dioleoyl-*sn*-glycero-3-phosphocholine (DOPC), 1,2-dioleoyl-3-trimethylammonium-propane (DOTAP)) were purchased from Avanti polar lipids. Mixed lipid stock solutions in 2.5 mg/mL and the number of G-net-gel (as collected from superhydrophobic layers; there were 800 units in a final adjusted volume of 50 μL) were gently mixed at room temperature for 2 h and then washed with 0.5x and 0.25x phosphate buffered saline (PBS) solutions as shown in Figure 4A.

mRNA Transcription Test. For the in vitro mRNA transcription test, a Hiscribe T7 in vitro transcription kit (NEB) was used to evaluate the mRNA transcripts generated from either commercial solution phase system (c-SPS) or G-net-gel. All mRNA products were further purified using a RNeasy Mini kit (Qiagen). mRNA transcription values (represented by fluorescence) were measured using Qubit RNA assay kits (Invitrogen). All experimental procedures were performed as described by the manufacturer.

Reverse Transcription−Polymerase Chain Reaction (RT-PCR) and Quantitative PCR (Real-Time PCR or qRT-PCR). mRNA obtained by in vitro transcription was purified using an RNeasy kit (Qiagen). The PrimeScript RT reagent kit (Takara Bio Inc.) was purchased to produce cDNA from the mRNA of either c-SPS or G-net-gel. SYBR Green Real-time PCR Master mix was purchased from TOYOBO CO. Ltd. Real-time PCR reactions were performed in an Applied Biosystems 7000 series to obtain a cDNA amplification plot. All assay protocols were performed as described by the manufacturer's guidelines. The forward primer sequence of AcGFP was 5′-TGACGGCAACTACAAGTCGC-3′ (20 bases), and the reverse primer sequence of AcGFP was 5′-GGCCTTGTCGGTCATGATG-TAC-3′ (22 bases).

■ RESULTS AND DISCUSSION

A new class of synthetic transcriptional organelles, termed proto-nuclei, is reported here. Artificially engineered nuclear constructs were created through a combination of structural DNA nanotechnology and liposome formulation. Briefly, a mixture of lipid components containing 95% DOPC and 5% DOTAP was combined with a network of genes and DNA blocks, resulting in a G-net-gel construct-supported lipid bilayers, which is able to act as a synthetic nucleus. A schematic of the system is shown in Figure 1. It was defined in this article that G-net-gel is a proto-nucleus as a genetic core, and, with lipid capping, G-net-gel-supported lipid bilayers become a synthetic and complete nucleus system. Since the nuclei of

dx.doi.org/10.1021/la303498k | *Langmuir* XXXX, XXX, XXX−XXX

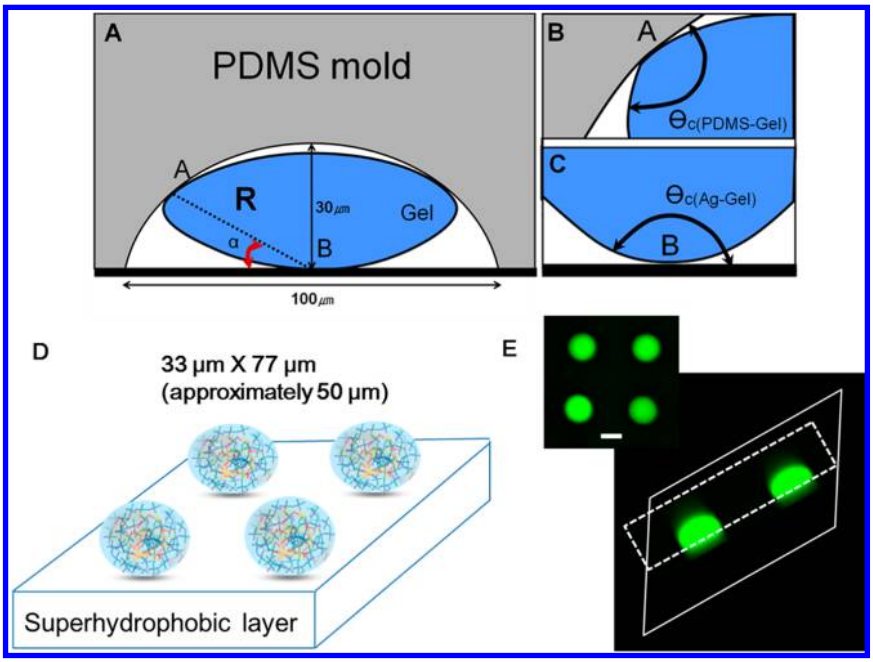

Figure 2. Fabrication and characterization of the G-net-gel matrix-supported lipid bilayers on a superhydrophobic surface. The fluid volume comes in contact with the bottom substrate and the PDMS mold while making the gel capsules (A). Before this fluid is cured in a mold, it must contact both the bottom glass and the top PDMS. Since this curing process is slower than the thermodynamic time scale (over 4 h), the fluid achieves equilibrium shape inside each mold. Its geometry is determined by the contact angles through the interactions between the three phases. As illustrated in (B), two contact angles were considered: θc(PDMS-Gel) is the contact angle between PDMS and gel fluids, and θc(Ag-Gel) is between the bottom substrate and the gel fluids as shown in (**C**). These two contact angles determine the angle, α, between the two contact points as $\alpha = \theta$c(PDMS-Gel)-θc(Ag-Gel) + $\pi/2$ derived from trivial geometric calculations. By measuring these two contact angles from separate experiments (θc(PDMS-Gel) = 100° and θc(Ag-Gel) = 150°), the width and height of the gel capsule (height (H): 32 μm width (W): 77 μm) was estimated. (D) Schematic drawing of spheroidal G-net-gel matrices on the superhydrophobic layer. (E) Fluorescence microscopic image of the G-net-gels on the superhydrophobic surface and confocal microscopic image of the G-net-gel on the superhydrophobic surface in the three-dimensional side view. The white dotted line represents the interface between the bottom and side views. Approximately 165 samples were used for each analysis. Note that the gel matrix shown in panel D shows a strong green emission when stained with the DNA-specific dye SYBR I (panel E).

most cells are either round or oval;[22] the proto-nuclei G-net-gel had a spheroidal shape, which was stabilized by beading up on a superhydrophobic layer. (The more detailed fabrication process of superhydrophobic layer is described in Figure S3.)

X-shaped DNA blocks were ligated with linear plasmid DNA encoding the target proteins and deposited into the PDMS micromold, as shown in Figure 2A–C. Precursor drops were then stamped onto the superhydrophobic surface with a contact angle of 161.5 degrees (Figure S3 and Table S1). This process resulted in a slightly damped spheroidal substance that was approximately 50 μm in diameter, as shown in Figure 2D. This process resulted in a spheroidal gel matrix yield greater than 75%. The gap difference in the hydrophobicity between the PDMS mold (~100 degrees) and the superhydrophobic surface (~150 degrees) promoted the adherence of the G-net-gel to the mold during the curing time. This may be why an oblate G-net-gel was obtained rather than a sphere. To validate this hypothesis, the contact angle of the G-net-gel precursor was measured, and a theoretical analysis was used to predict the resulting shapes. Once precursor-containing plasmid, DNA blocks, and buffer were added, the surface tension was 70 dyn/cm, which was slightly less than the surface tension of distilled water (72 dyn/cm), indicating that the G-net-gel decreased the tension at the interface due to the addition of polymer components. The width and height of the gel core material were then estimated. The theoretical height of the G-net-gel was approximately 32 μm, and the width was about 77 μm. Thus, the G-net-gel shape was determined to be an oblate spheroid, as shown in Figure 2A–D. After being stained with SYBR-I as a DNA-specific dye, the spheroidal G-net-gel was observed in strong green color emission, as shown in Figure 2E.

The parameters governing protein production of the G-net-gel as a proto-nucleus were first investigated and optimized, which included the number of G-net-gel spheroids, the concentration of a proof-model plasmid in the scaffold, and the molar ratio between the X-DNA building blocks and the gene. Aqueorea coerulescens green fluorescent protein (AcGFP) was used as a model protein, and wheat germ lysates provided from Roche were used as a cell-free system. The number of units used in the reaction was varied, and the plasmid (gene) amount was fixed at 7.8 pg per unit. G-net-gel of 100, 200, 400, and 800 units was used, which corresponded to plasmid amounts of 0.78, 1.56, 2.25, and 3 ng, respectively. As a control, the same amount of plasmid was used in a c-SPS. The protein expression results shown in Figure 3A illustrate that the G-net-gel exhibited a higher efficiency and a better yield than the c-SPS control under each condition. In particular, the G-net-gel consisting of 800 units produced approximately 0.15 μg per ml within 24 h, which is equivalent to the expression efficiency of 2.5 μg protein per 1 μg plasmid, or 3 μg/mL. This represents a 20-fold enhancement in both yield and efficiency over the c-SPS control (Figure 3B). To further explore the mechanism of the G-net-gel system, the X-DNA/gene ratio was varied from 1000:1 to 7000:1 by varying the X-DNA amount while maintaining the number of units and the gene concentration. Figure 3C shows that the optimal X-DNA/

dx.doi.org/10.1021/la303498k | *Langmuir* XXXX, XXX, XXX–XXX

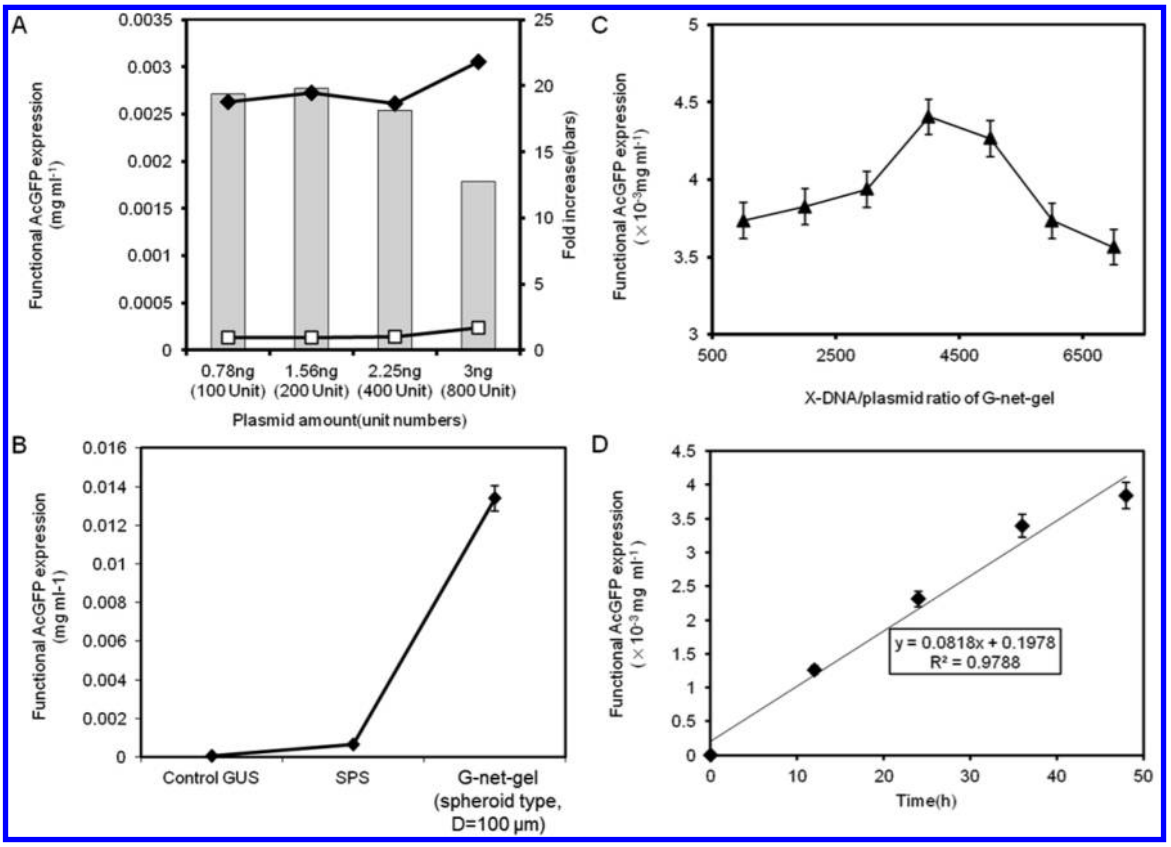

Figure 3. Functional AcGFP expression in the G-net-gel under different conditions. (A) AcGFP expression by the number of spheroid units in the reaction (diamond shapes). The same amount of plasmid was used in the SPS control (open squares). Bars indicate the fold increase in the functional protein expression of G-net-gels over the SPS controls. (B) Comparison between the control GUS, SPS (AcGFP), and spheroid type G-net-gel (diameter ~100 μm). RFU was measured and converted to weight concentration for each sample. (C) Functional AcGFP expression in the G-net-gel at different X-DNA/plasmid ratios. (D) Time course of functional AcGFP expression in the spheroid-type G-net-gel. For B–D, approximately 800 G-net-gels were used for analysis. As a control, the same amount of plasmid was used in a c-SPS.

gene ratio for AcGFP expression was 4000:1. These results suggest that the G-net-gel can tolerate a wide range of cross-linker/gene ratios. Protein expression was monitored as a function of reaction time in order to better understand the kinetic behavior of this system, and AcGFP expression was found to increase linearly with reaction time (Figure 3D). The G-net-gel continuously produced protein for more than 36 h, whereas the c-SPS reached a plateau after only 12 h. The speed (slope) of gene expression using the G-net-gel was approximately 70-fold faster than that of the c-SPS in the first 12 h. Thus, the G-net-gel showed greatly improved kinetic behavior over the c-SPS. In addition, the images shown in Figure S4 clearly demonstrate that the G-net-gel produced significantly more functional protein than the c-SPS.

To mimic the natural nucleus system, which is composed of a nucleus membrane and genomic DNA, spheroidal G-net-gel matrices were fully enclosed with a lipid membrane supporter consisting of bimodular lipid components (DOPC and DOTAP). This system, a G-net-gel matrix-supported bilayer, was designated a synthetic nucleus system to differentiate it from the proto-nuclei G-net-gel system. Lipid membranes 4 nm thick were successfully manufactured at the gel matrix surface (Figure 4A,B). A round shaped gene networking matrix-supported bilayer was observed (Figure 4A,B). In fluorescent sectional images, a red emission corresponding to the lipid component was clearly seen to surround the strong green colors corresponding to the gene matrix. The outer barrier of the gel matrix was fully enclosed by the lipid mixture. Even at approximately 100% coverage (Figure S5), the hydrogel that was encapsulated with lipid components easily cracked into lipid-supported gel pieces during preparation, but once treated using a budding-off method that was developed in our lab,[23] a microscaled gel network-supported bilayer was obtained.

To prove that this system, like a natural nucleus, was able to produce mRNA precursors through transcription, a primary transcription mixture containing T7 RNA polymerase, NTP mixture, ATP, and solution buffer was combined in the gel matrix during in situ gelation. All cases resulted in complete gelation, irrespective of the species added (Figure 4C). When mRNA efficiency was evaluated relative to the control groups, the G-net-gel matrix system, including complete transcription components, was shown to produce the greatest amount of mRNA (Figure 4C, Case 3). The level of mRNA transcription of the G-net-gel was 2-fold greater than that of the c-SPS, but the transcription level of the G-net-gel-supported bilayer was lower. As shown in Figure 4, the mRNA transcripts generated in the G-net-gel may not be permeable to the outer lipid envelope. When the supporting lipid membranes were permeabilized using Triton X-100, an mRNA level similar to that of the unsupported G-net-gel was obtained (Figure 4C, Case 3).

In addition to the mRNA fluorescence studies, qRT-PCR was used to confirm that cDNA amounts were greater using the gene-networked matrix system relative to the c-SPS control

dx.doi.org/10.1021/la303498k | Langmuir XXXX, XXX, XXX–XXX

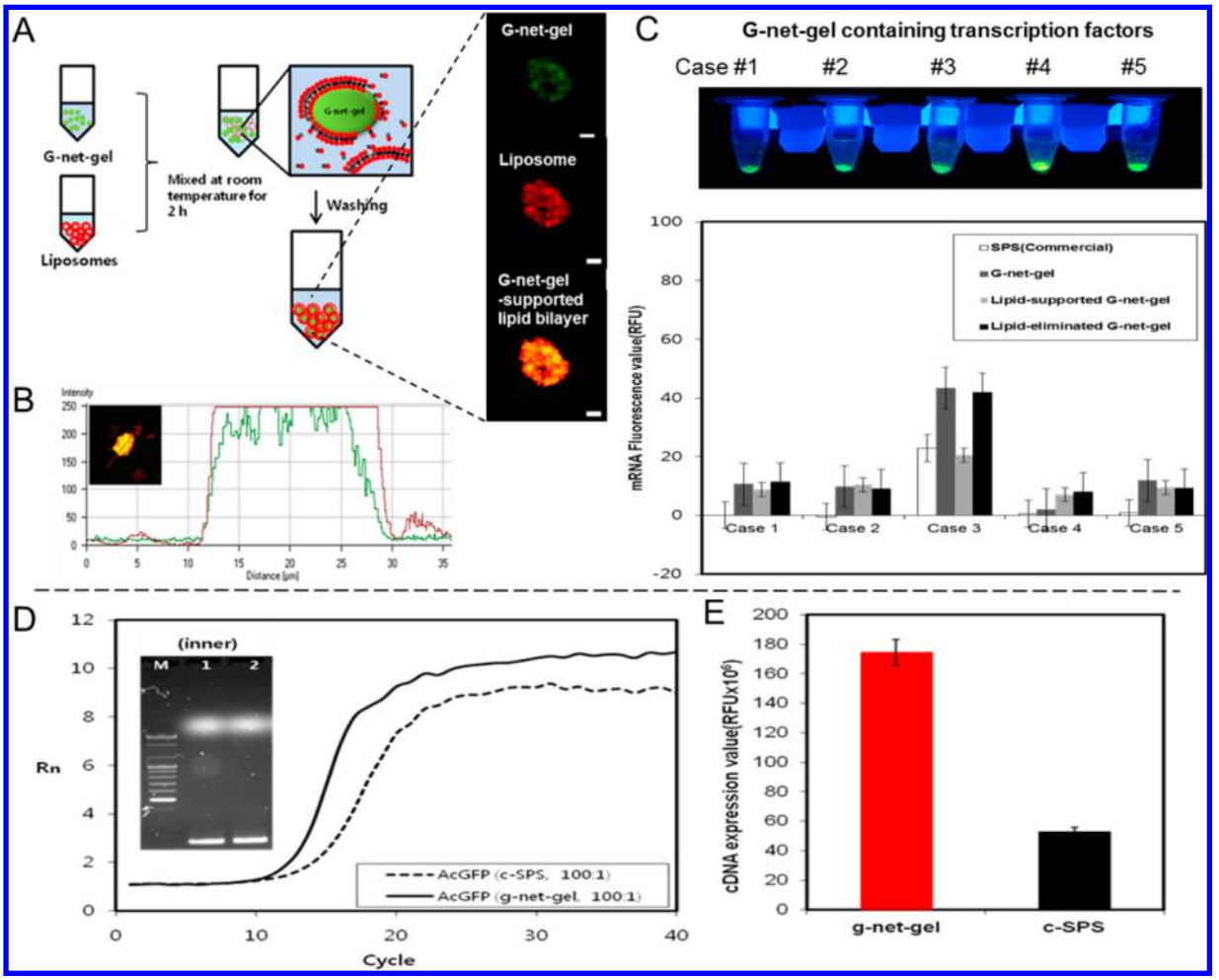

Figure 4. Fabrication and characterization of the synthetic nucleus system, gene-networked gel matrix-supported lipid bilayer system. (A) Fabrication processing of the synthetic nucleus system from G-net-gel collected from the superhydrophobic layer. The system is based on the combination of a gene-networked hydrogel (G-net-gel) as a core-nucleus and an outer lipid membrane. (B) Profiling plot of the G-net-gel-supported lipid bilayer, synthetic nucleus system. (C) In situ testing of transcription factor encapsulation and in vitro mRNA transcription measurement. Five conditions were tested: Case 1 was a G-net-gel control; Case 2 was G-net-gel + T7 RNA polymerase +10 x transcription buffer; Case 3 was G-net-gel + T7 RNA polymerase +10 x transcription buffer +20 x NTP mixture; Case 4 was G-net-gel +20 x NTP mixture; Case 5 was G-net-gel + T7 RNA polymerase. All transcription factors were encapsulated into the G-net-gel as shown in the figure. mRNA was purified using a RNeasy Mini kit (Qiagen). 0.01% Triton X-100 (total volume of 20 μL) was treated with G-net-gel-supported lipid bilayers for 6 h (Statistically analyzed by Student's t test: $p < 0.05$). (C) Confocal microscopic images of the synthetic nucleus system (magnification of 20 × 10, scale bar =5 μm). Note that the red color in the middle of Figure originated from the Texas Red-labeled lipid inserted into the lipid components and the green color came from the SYBR-I stained DNAs. (D) cDNA amplification plot where each line is a plot of cDNA amplification generated by G-net-gel. The dotted line indicates the amplification generated by SPS, and the inset (inner) shows the qPCR products: 100bp DNA ladder (M), AcGFP qPCR product from SPS (Lane 1), AcGFP qPCR product from G-net-gel (Lane 2). (E) cDNA expression quantitative plot as evaluated by the ddCt method. As a control, the same amount of plasmid was used in a c-SPS.

(Figure 4D,E). The cycle threshold (Ct) value for the G-net-gel and c-SPS were 11.51 and 13.05, respectively, indicating that the mRNA of the G-net-gel was more productive than that of the c-SPS. Provided that the PCR efficiency was equal in all cases, the relative quantitative values of cDNA expression can be evaluated using the ΔΔCt method (For more detail, see Supporting Information). The quantitative values of cDNA were recalculated as approximately 17.5×10^7 and 5.3×10^7 for the G-net-gel and c-SPS, respectively (Figure 4D and E). The enhanced cDNA of the G-net-gel and the cross-linked exogene structures may be the principal factors of greater expression. Thus, this system could be used as a novel proto-nucleus system.

CONCLUSIONS

Our study demonstrated that a synthetic nucleus system can be simply manufactured via both structural DNA nanotechnology and liposome formulation. According to the strategy of rational design, the core gel networks, the G-net-gels, were shown to have the expected spheroidal shape. This shape was formed between the hydrophobic layers and the superhydrophobic substrate. Lastly, an artificial nucleus was built that had a three-dimensional architecture consisting of three major subdivisions: an outer membrane, genomic DNA ligated to a DNA block, and transcription components and under transcription environments; it produced a mRNA transcript as did the natural nucleus.

This system is still far from a real nucleus system as the size of the artificial system (approximately 50 μm diameter) is

dx.doi.org/10.1021/la303498k | Langmuir XXXX, XXX, XXX–XXX

significantly larger than that of the natural system (approximately 1−5 μm diameter).[24] In addition, the artificial system has no nuclear transporters to deliver the components necessary for gene metabolism, thus resulting in a lower transcription efficiency (Figure 4C) as enclosed by lipid membranes in this research. There are several issues to be considered in the construction of an artificial system: (1) Is there a regulatory or replication machinery needed for gene? (2) Is there a signaling system for gene regulation/replication? (3) Is there the capability for multitransgene repositioning? Based on these questions, attempts to assemble synthetic nucleus systems should be studied using (1) unrestrained surface functionalization via several chemical methods and (2) rearrangement of several transgenes to predetermined positions in order to construct regularly patterned DNA templates. Nonetheless, this nucleus system is very promising, as it is the first synthetic nuclear system to follow biomimetic engineering strategies. It will be challenging to test the many unresolved problems and hypotheses. Future bioapplications will be aided by determining how genomes are spatially organized and inherited in vitro. For example, an artificial gene matrix could act as a substitute for a malfunctioning cell nucleus, which could be used in gene therapeutics. Conventional gene therapy, where genomic internalization into the nuclear membrane remains a serious issue, could be advanced through the development of synthetic nucleus substitutes which contain therapeutic transgenes. Once associated with a protocell as a nanocarrier construct source[25−29] and a synthetic yeast genome system,[30] this system might further evolve into a platform for an artificial cell for in vivo diagnostics. In addition, this approach could be used for the development of DNA chips, electronic sensors, stimulative drug delivery systems, and protein therapy.[31−33]

■ ASSOCIATED CONTENT

Ⓢ Supporting Information

Experimental procedures regarding the used X-DNA sequence and evaluation of cDNA expression by the ΔΔCt method. Experimental results regarding surface morphology observation through SEM about the superhydrophobic layers, fabrication processing of superhydrophobic surfaces, design concept of the new PDMS mold for production of spheroidal gel matrices, SDS-polyacrylamide gel electrophoresis assays for the confirmation of AcGFP, GDNF, and TRAIL protein expression in both G-net-gel and c-SPS, confocal microscopic images of the G-net-gels encapsulated in the mixed lipid moieties, contact angle measurements of the superhydrophobic layers, and projection on the horizontal plane of a Z-stack movie illustrating a G-net-gel matrix. This material is available free of charge via the Internet at http://pubs.acs.org

■ AUTHOR INFORMATION

Corresponding Author

*E-mail: sh.um@skku.edu.

Notes

The authors declare no competing financial interest.

■ ACKNOWLEDGMENTS

We thank Prof. Gun Young Jung and Prof. Sung Ju Park for providing ZnO nanoparticles and surface modifications and Dr. Ae-Kyoung Kim for kindly providing technical assistance with RT-PCR. This study was mainly supported by a grant from the Korea Health Technology R&D Project of the Ministry of Health & Welfare of the Republic of Korea (Grant No. A110552) and by the National Foundation of Korea (NRF) grant funded by the Korean Government (MEST) (No. 20100007782 and 20100026793; Midcareer Researcher Program).

■ REFERENCES

(1) Lowe, A. R.; Siegel, J. J.; Kalab, P.; Siu, M.; Weis, K.; Liphardt, J. T. Selectivity mechanism of the nuclear pore complex characterized by single cargo tracking. *Nature* **2010**, *467*, 600−603.

(2) Grünwald, D.; Singer, R. H.; Rout, M. Nuclear export dynamics of RNA−protein complexes. *Nature* **2011**, *475*, 333−341.

(3) Ewers, H.; Smith, A. E.; Sbalzarini, I. F.; Lilie, H.; Koumoutsakos, P.; Helenius, A. Single-particle tracking of murine polyoma virus-like particles on live cells and artificial membranes. *Proc. Natl. Acad. Sci. U.S.A.* **2005**, *102*, 17669−17674.

(4) Cohen, I. R. Real and artificial immune systems: Computing the state of the body. *Nat. Rev. Immunol.* **2007**, *7*, 569−574.

(5) Kim, J. V.; Latouche, J. B.; Rivière, I.; Sadelain, M. The ABCs of artificial antigen presentation. *Nat. Biotechnol.* **2004**, *22*, 403−410.

(6) Dreyfus, R.; Baudry, J.; Roper, M. L.; Fermigier, M.; Stone, H. A.; Bibette, J. Microscopic artificial swimmers. *Nature* **2005**, *437*, 862−865.

(7) Noireaux, V.; Libchaber, A. A vesicle bioreactor as a step toward an artificial cell assembly. *Proc. Natl. Acad. Sci. U.S.A.* **2004**, *101*, 17669−17674.

(8) Noireaux, V.; Maeda, Y. T.; Libchaber, A. Development of an artificial cell, from self-organization to computation and self-reproduction. *Proc. Natl. Acad. Sci. U.S.A.* **2011**, *108*, 3473−3480.

(9) Yoo, J. W.; Irvine, D. J.; Discher, D. E.; Mitragotri, S. Bio-inspired, bioengineered and biomimetic drug delivery carriers. *Nat. Rev. Drug Discov.* **2011**, *10*, 521−535.

(10) Osada, K.; Oshima, H.; Kobayashi, D.; Doi, M.; Enoki, M.; Yamasaki, Y.; Kataoka, K. Quantized folding of plasmid DNA condensed with block catiomer into characteristic rod structures promoting transgene efficiency. *J. Am. Chem. Soc.* **2010**, *132*, 12343−12348.

(11) Jovanovic-Talisman, T.; Tetenbaum-Novatt, J.; McKenney, A. S.; Zilman, A.; Peters, R.; Rout, M. P.; Chait, B. T. Artificial nanopores that mimic the transport selectivity of the nuclear pore complex. *Nature* **2009**, *457*, 1023−1027.

(12) Kowalczyk, S. W.; Kapinos, L.; Blosser, T. R.; Magalhães, T.; van Nies, P.; Lim, R. Y.; Dekker, C. Single-molecule transport across an individual biomimetic nuclear pore complex. *Nat. Nanotechnol.* **2011**, *6*, 433−438.

(13) Lanctôt, C.; Cheutin, T.; Cremer, M.; Cavalli, G.; Cremer, T. Dynamic genome architecture in the nuclear space regulation of gene expression in three dimensions. *Nat. Rev. Genet.* **2007**, *8*, 104−115.

(14) Feldkamp, U.; Niemeyer, C. M. Rational design of DNA nanoarchtectures. *Angew. Chem., Int. Ed.* **2006**, *45*, 1856−1876.

(15) Pinheiro, A. V.; Han, D.; Shih, W. M.; Yan, H. Challenges and opportunities for structural DNA nanotechnology. *Nat. Nanotechnol.* **2011**, *6*, 763−772.

(16) Um, S. H.; Lee, J. B.; Park, N.; Kwon, S. Y.; Umbach, C. C.; Luo, D. Enzyme-catalysed assembly of DNA hydrogel. *Nat. Mater.* **2006**, *5*, 797−801.

(17) Park, N.; Um, S. H.; Funabashi, H.; Xu, J.; Luo, D. A cell-free protein-producing gel. *Nat. Mater.* **2009**, *8*, 432−437.

(18) Jiang, L.; Zhao, Y.; Zhai, J. A lotus-leaf-like superhydrophobic surface: A porous microsphere/nanofiber composite film prepared by electrohydrodynamics. *Angew. Chem. Int. Ed.* **2004**, *43*, 4338−4341.

(19) Bae, S. J.; Song, W. C.; Song, H.; Jung, G. Y.; Um, S. H. New superhydrophobic layer for a spherical DNA hydrogel. Submitted.

(20) Tuteja, A.; Choi, W.; Ma, M.; Mabry, J. M.; Mazzella, S. A.; Rutledge, G. C.; McKinley, G. H.; Cohen, R. E. Designing superoleophobic surfaces. *Science* **2007**, *318*, 1618−1622.

(21) Huang, Y. F.; Chattopadhyay, S.; Jen, Y. J.; Peng, C. Y.; Liu, T. A.; Hsu, Y. K.; Pan, C. L.; Lo, H. C.; Hsu, C. H.; Chang, Y. H.; Lee, C.

S.; Chen, K. H.; Chen, L. C. Improved broadband and quasiomnidirectional anti-reflection properties with biomimetic silicon nanostructures. *Nat. Nanotechnol.* **2007**, *2*, 770−774.
(22) Webster, M.; Witkin, K. L.; Cohen-Fix, O. Sizing up the nucleus: Nuclear shape, size and nuclear-envelope assembly. *J. Cell Sci.* **2009**, *122*, 1477−1486.
(23) Bae, S. J.; Jung, S.; Um, S. H. Budding dynamics of the lipid membrane. *J. Nanosci. Nanotechnol.* **2011**, *11*, 6172−6176.
(24) Lanctôt, C.; Cheutin, T.; Cremer, M.; Cavalli, G.; Cremer, T. Dynamic genome architecture in the nuclear space: Regulation of gene expression in three dimensions. *Nat. Rev. Genet.* **2007**, *8* (2), 104−115.
(25) Ashley, C. E.; Carnes, E. C.; Phillips, G. K.; Padilla, D.; Durfee, P. N.; Brown, P. A.; Hanna, T. N.; Liu, J.; Phillips, B.; Carter, M. B.; Carroll, N. J.; Jiang, X.; Dunphy, D. R.; Willman, C. L.; Petsev, D. N.; Evans, D. G.; Parikh, A. N.; Chackerian, B.; Wharton, W.; Peabody, D. S.; Brinker, C. J. The targeted delivery of multicomponent cargos to cancer cells by nanoporous particle-supported lipid bilayers. *Nat. Mater.* **2011**, *10*, 389−397.
(26) Liu, J.; Jiang, X.; Ashley, C.; Brinker, C. J. Electrostatically mediated liposome fusion and lipid exchange with a nanoparticle-supported bilayer for control of surface charge, drug containment, and delivery. *J. Am. Chem. Soc.* **2009**, *131*, 7567−7569.
(27) Liu, J.; Stace-Naughton, A.; Jiang, X.; Brinker, C. J. Porous nanoparticle supported lipid bilayers (Protocells) as delivery vehicles. *J. Am. Chem. Soc.* **2009**, *131*, 1354−1355.
(28) Liu, J.; Stace-Naughton, A.; Brinker, C. J. Silica nanoparticle supported lipid bilayers for gene delivery. *Chem. Commun.* **2009**, *34*, 5100−5102.
(29) Prata, C. A.; Li, Y.; Luo, D.; McIntosh, T. J.; Barthelemy, P.; Grinstaff, M. W. A new helper phospholipid for gene delivery. *Chem. Comnun.* **2008**, *13*, 1566−1568.
(30) Dymond, J. S.; Richardson, S. M.; Coombes, C. E.; Babatz, T.; Muller, H.; Annaluru, N.; Blake, W. J.; Schwerzmann, J. W.; Dai, J.; Lindstrom, D. L.; Boeke, A. C.; Gottschling, D. E.; Chandrasegaran, S.; Bader, J. S.; Boeke, J. D. Synthetic chromosome arms function in yeast and generate phenotypic diversity by design. *Nature* **2011**, *477*, 471−476.
(31) Grünwald, D.; Singer, R. H. In vivo imaging of labeled endogenous *β*-action mRNA during nucleocyto plasmic transport. *Nature* **2010**, *467*, 604−607.
(32) Son, S.; Kim, G.; Singha, K.; Park, S.; Ree, M.; Kim, W. J. Artificial cell membrane-mimicking nanostructure facilitates efficient gene delivery through fusogenic interaction with the plasma membrane of living cells. *Small* **2011**, *7*, 2991−2997.
(33) Hirayama, T.; Van de Bittner, G. C.; Gray, L. W.; Lutsenko, S.; Chang, C. J. Near-infrared fluorescent sensor for in vivo copper imaging in a murine Wilson disease model. *Proc. Natl. Acad. Sci. U.S.A.* **2012**, *109*, 2228−2233.